

Supporting Information for:

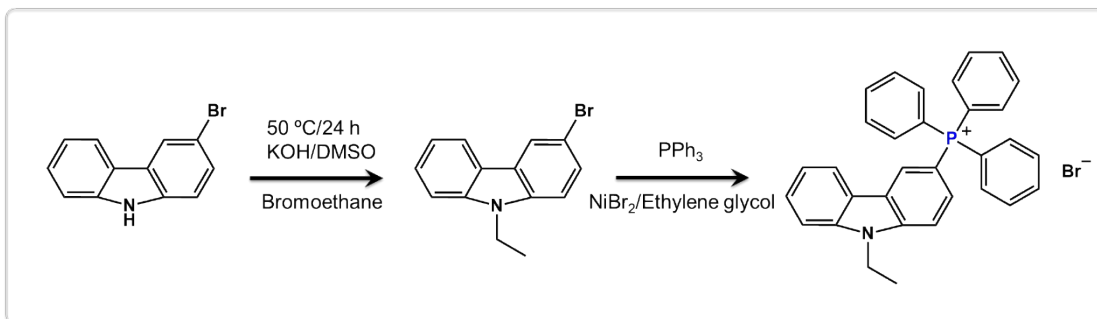
**Surface Passivation of Perovskite Thin Films by  
Phosphonium Halides for Efficient and Stable Solar Cells**

Qingquan He,<sup>a</sup> Michael Worku,<sup>b</sup> Liangjin Xu,<sup>a</sup> Chenkun Zhou,<sup>c</sup> Sandrine Lteif,<sup>a</sup> Joe Schlenoff<sup>a</sup>  
and Biwu Ma<sup>\*a,b,c</sup>

<sup>a</sup> Department of Chemistry and Biochemistry, Florida State University, Tallahassee, FL 32306,  
USA. E-mail: [bma@fsu.edu](mailto:bma@fsu.edu)

<sup>b</sup> Materials Science and Engineering Program, Florida State University, Tallahassee, FL 32306,  
USA

<sup>c</sup> Department of Chemical and Biomedical Engineering, FAMU-FSU College of Engineering,  
Tallahassee, FL 32310, USA



**Scheme S1.** Illustration of the synthesis procedures of TCPBr.

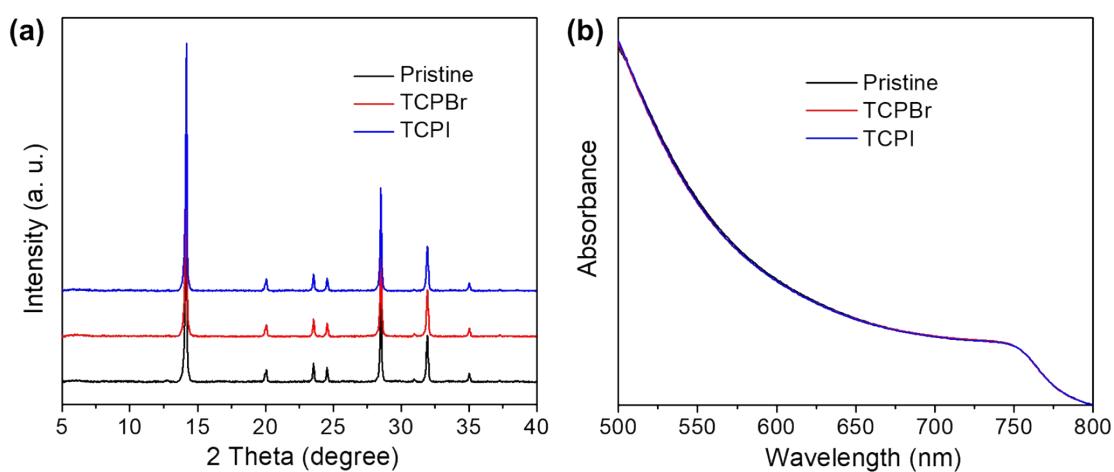


**Fig. S1** (a) XRD patterns and (b) UV-Vis spectra of the different perovskite thin films with the thickness of 450 nm (general films).

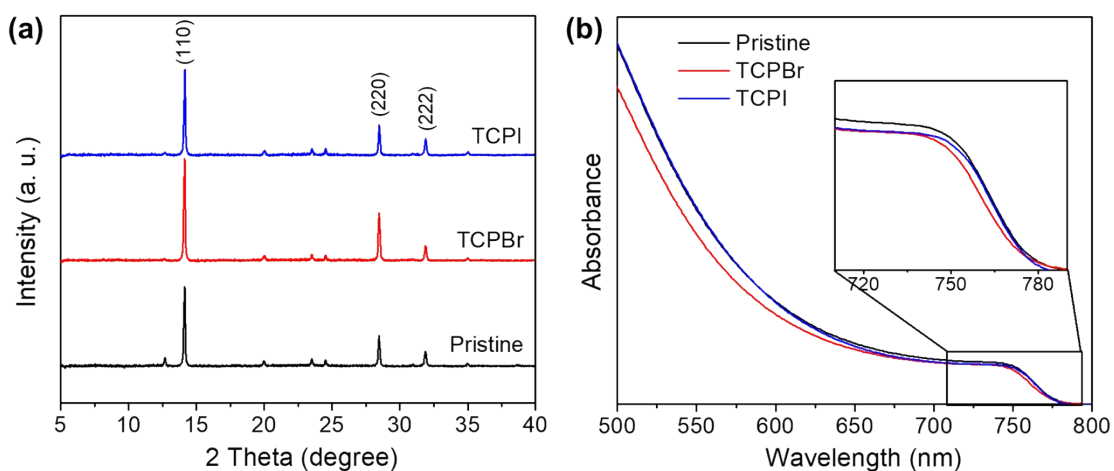


**Fig. S2** (a) XRD patterns and (b) UV-Vis spectra of the different perovskite thin films with the thickness of 100 nm (thinner films). Inset of (b) is a zoom-in view near the absorption edge.

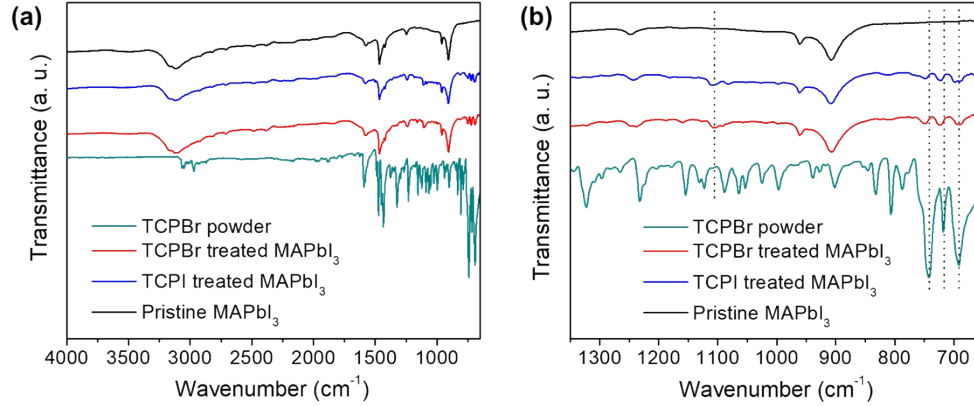


**Fig. S3** (a) FT-IR and (b) zoom-in view spectra of TCPBr powder, TCPBr treated, TCPI treated, and pristine MAPbI<sub>3</sub>.

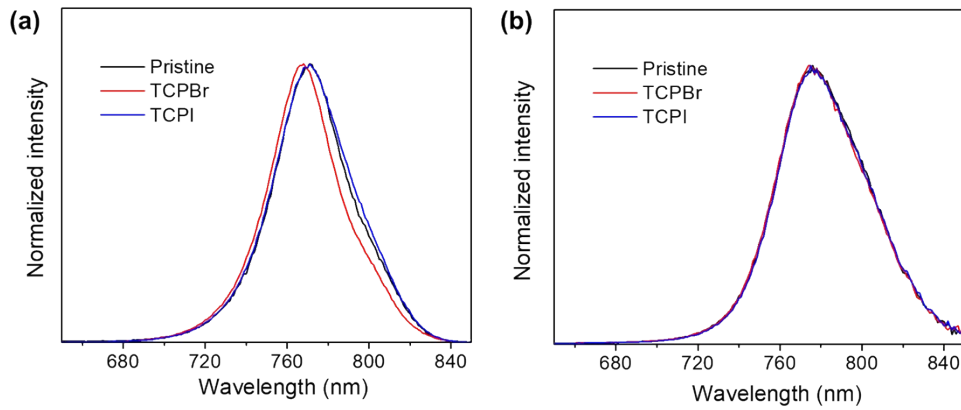


**Fig. S4** Normalized PL spectra of the MAPbI<sub>3</sub> films treated with different organic halide salts scanned from (a) front and (b) back side.

**Table S1** Fitted parameters for time resolved PL decay of perovskite films (architecture: glass/perovskite). A biexponential decay model was used.

Sample	$\tau_1$ (ns)	$\tau_2$ (ns)	$A_1$ (%)	$A_2$ (%)	$\tau_{ave}$ (ns)
Pristine	12.4	79.4	30.2	69.8	75.2
TCPBr	13.5	531.1	5.4	94.6	530.2
TCPI	13.2	422.2	8.9	91.1	421.0

**Table S2** Fitted parameters for time resolved PL decay of devices based on different perovskite films (architecture: glass/perovskite/*spiro*-OMeTAD). A biexponential decay model was used.

Sample	$\tau_1$ (ns)	$\tau_2$ (ns)	$A_1$ (%)	$A_2$ (%)	$\tau_{ave}$ (ns)
Pristine	5.6	36.1	89.4	10.6	18.8
TCPBr	4.9	22.1	83.4	16.6	13.0
TCPI	5.4	27.4	84.8	15.2	15.9

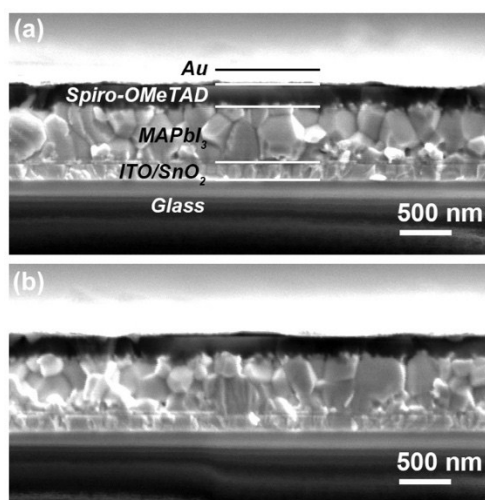


**Fig. S5** Cross-sectional SEM images of the planar n-i-p PSCs based on (a) pristine and (b) TCPBr ( $0.6 \text{ mg mL}^{-1}$ ) treated MAPbI<sub>3</sub> thin films.

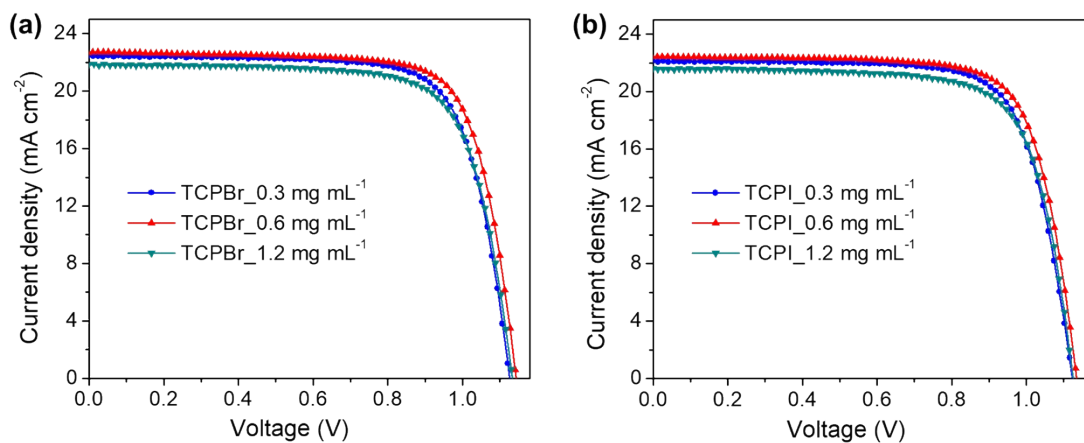


**Fig. S6**  $J$ - $V$  curves of the best-performing devices based on the perovskite thin films passivated by (a) TCPBr and (b) TCPI with different concentration.

**Table S3** Photovoltaic characteristics of the best-performing devices based on TCPBr treated perovskites.

Sample	$J_{SC}$ (mA/cm <sup>2</sup> )	$V_{OC}$ (V)	FF	PCE (%)
0.3 mg mL <sup>-1</sup>	22.40	1.12	0.76	19.03
0.6 mg mL <sup>-1</sup>	22.63	1.14	0.78	20.13
1.2 mg mL <sup>-1</sup>	21.77	1.13	0.76	18.69

**Table S4** Photovoltaic characteristics of the best-performing devices based on TCPI treated perovskites.

Sample	$J_{SC}$ (mA/cm <sup>2</sup> )	$V_{OC}$ (V)	FF	PCE (%)
0.3 mg mL <sup>-1</sup>	22.09	1.12	0.75	18.63
0.6 mg mL <sup>-1</sup>	22.42	1.13	0.77	19.41
1.2 mg mL <sup>-1</sup>	21.51	1.12	0.76	18.27

**Table S5** Photovoltaic characteristics of the best-performing devices.

Sample <sup>a</sup>	$J_{SC}$ (mA/cm <sup>2</sup> )	$V_{OC}$ (V)	FF	PCE (%)
Pristine (R-F)	22.15	1.11	0.75	18.52
Pristine (F-R)	22.11	1.08	0.69	16.45
TCPBr (R-F)	22.63	1.14	0.78	20.13
TCPBr (F-R)	22.54	1.13	0.75	19.04
TCPI (R-F)	22.42	1.13	0.77	19.41
TCPI (F-R)	22.36	1.12	0.73	18.32

a: the R-F is the reverse scan (1.2 V  $\rightarrow$  0 V), the F-R is forward scan (0 V  $\rightarrow$  1.2 V)

**Table S6** Average photovoltaic parameters of PSCs based on different perovskite layer.

Sample	$J_{SC}$ (mA/cm <sup>2</sup> )	$V_{OC}$ (V)	FF	PCE (%)
Pristine	21.59	1.10	0.73	17.50
TCPBr	22.49	1.13	0.76	19.31
TCPI	22.11	1.12	0.75	18.62

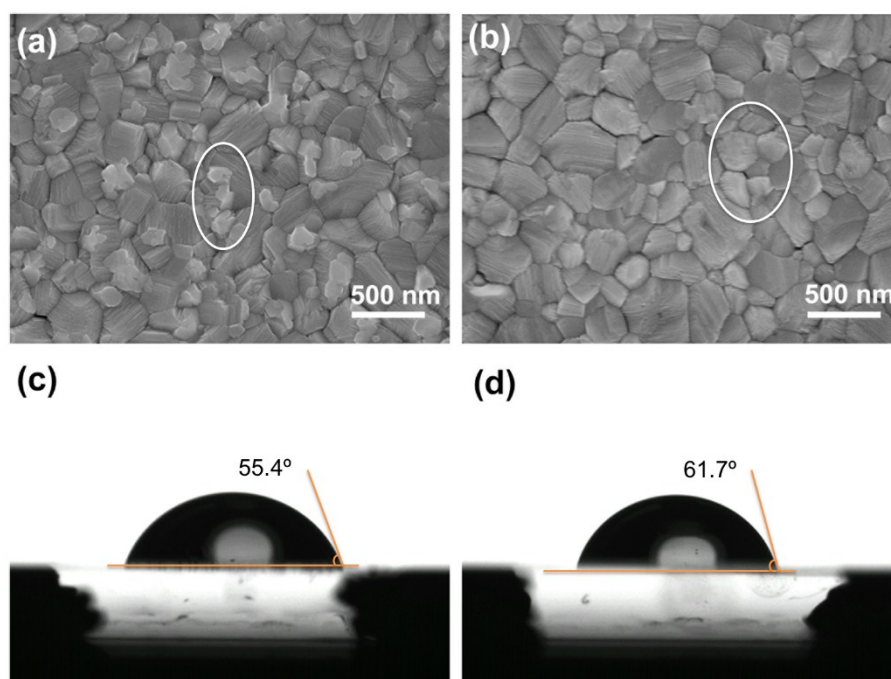


**Fig. S7** Top-view SEM images and (a) 0.6 mg mL<sup>-1</sup> PEAI and (b) 1.2 mg mL<sup>-1</sup> PEAI treated perovskite thin films. Contact angle between water and the (c) 0.6 mg mL<sup>-1</sup> PEAI and (d) 1.2 mg mL<sup>-1</sup> PEAI treated perovskite thin films.

Additional control experiments based on phenethylammonium iodide (PEAI) passivation agent were performed under the same conditions. The top-view SEM images of PEAI treated MAPbI<sub>3</sub> thin films are shown in Fig. S7a,b. After treating with 0.6 mg mL<sup>-1</sup> of PEAI, some new grains appeared in white oval (Fig. S7a), which are different from the pristine and TCPBr treated samples. The new formed materials are not fully covering the surface of MAPbI<sub>3</sub> crystallites. By increasing the concentration of PEAI to 1.2 mg mL<sup>-1</sup>, the size of these new generated grains grew larger

instead of covering the MAPbI<sub>3</sub> surface (in white oval, Fig. S7b). Unlike the TCPBr treated samples, most of the perovskite crystallites and grain boundaries are still can be observed clearly after passivating with PEAI, indicating the lower passivation effectiveness of PAEI for MAPbI<sub>3</sub>. We also measured the contact angle between water and PEAI treated perovskite thin films. Fig. S7c and S7d show the contact angles increased from 29.9° (pristine MAPbI<sub>3</sub> thin film, see Fig. 1h in main text) to 55.4° and 61.7° for 0.6 and 1.2 mg mL<sup>-1</sup> PEAI treated samples, respectively. The contact angles of all PEAI passivated samples are lower than those of TCPBr and TCPI, which might affect the stability of perovskite thin films and devices.

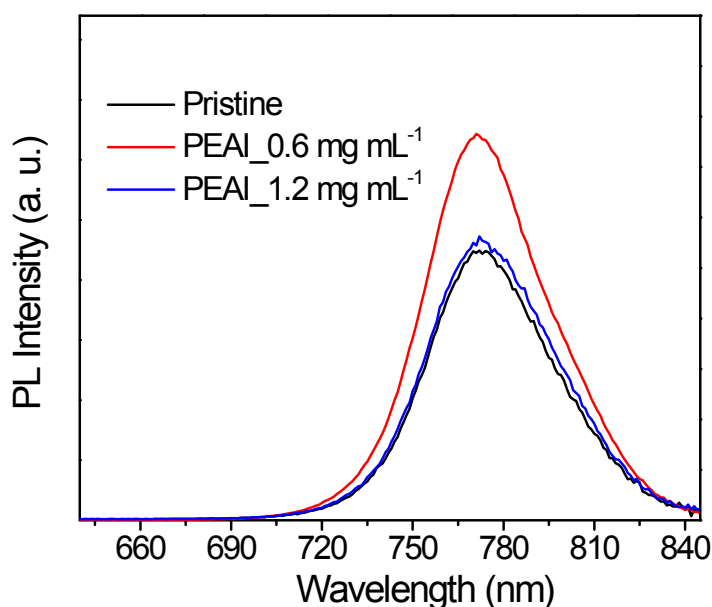


**Fig. S8** Steady PL spectra of the pristine and PEAI passivated perovskite thin films.

Steady-state PL spectra of the passivated perovskite thin films were recorded to reveal the influences of PEAI treatment on the photophysical properties. As shown in Fig. S8, the perovskite thin film treated by 0.6 mg mL<sup>-1</sup> PEAI exhibited higher peak intensity than that of pristine MAPbI<sub>3</sub> thin film, suggesting that PEAI could passivate surface defects and reduce nonradiative recombination to some extent.<sup>1, 2</sup> The decreasing of peak density after treating by a higher concentration PEAI (1.2 mg mL<sup>-1</sup>) could be ascribed to the possible formation of new defects.

Planar n-i-p PSCs were fabricated and tested to further investigate the impact of PEAI treatment. The fabrication procedures were kept the same, except varying the perovskite layers. The  $J$ - $V$  curves and photovoltaic parameters for the best performing devices based on pristine and PEAI treated perovskite thin films are shown in Fig. S9 and Table S7. The PSCs based on pristine MAPbI<sub>3</sub> gave a PCE of 18.46% with a  $J_{SC}$  of 22.09 mA cm<sup>-2</sup>, a  $V_{oc}$  of 1.11 V, and an FF of 0.75, respectively. The device fabricated with 0.6 mg mL<sup>-1</sup> PEAI treated perovskite exhibited an  $J_{SC}$  of 22.37 mA cm<sup>-2</sup>, a  $V_{OC}$  of 1.12 V, an FF of 0.75, subsequently an enhanced PCE to 18.83%. While the devices based on 1.2 mg mL<sup>-1</sup> of PEAI treated perovskite films gave the PCE of 18.49. These results indicate that the treatment of PEAI can improve the properties of MAPbI<sub>3</sub> thin films and PSCs, but the passivation effectiveness of PEAI is still lower than that of TCPBr and TCPI. These contents have been added and highlighted in our revised manuscript.

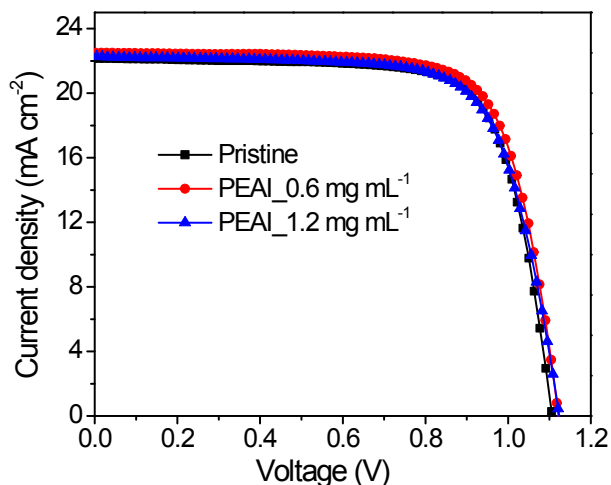


**Fig. S9**  $J$ - $V$  curves of the best-performing devices based on the perovskite thin films passivated by PEAI with different concentration.



**Table S7** Photovoltaic characteristics of the best-performing devices based on PEAI treated perovskites.

Sample	$J_{SC}$ (mA/cm <sup>2</sup> )	$V_{OC}$ (V)	FF	PCE (%)
Pristine	22.09	1.11	0.75	18.46
0.6 mg mL <sup>-1</sup>	22.37	1.12	0.75	18.83
1.2 mg mL <sup>-1</sup>	22.25	1.12	0.74	18.49

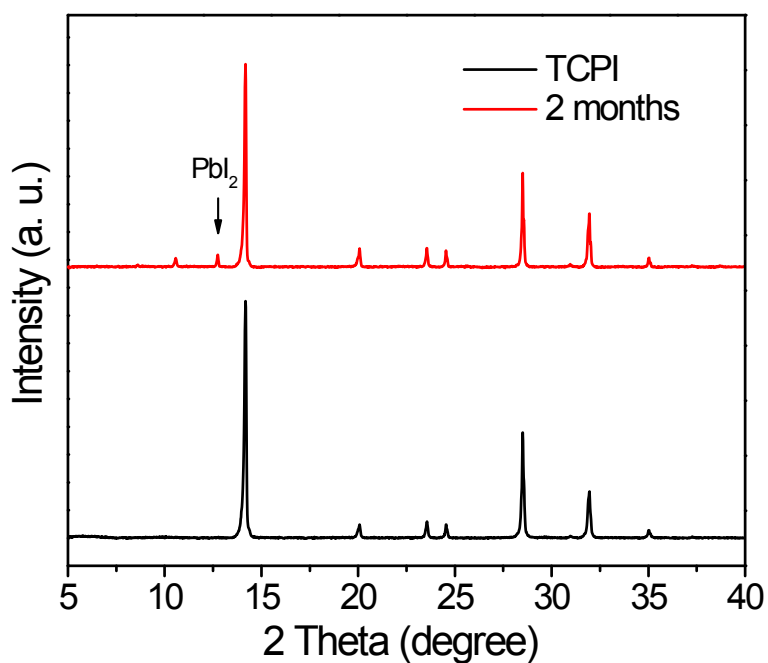


**Fig. S10** XRD patterns of TCPI treated perovskite thin films before and after exposure to ambient conditions with 60-80% RH at room temperature

## References

1. W. Q. Wu, Z. B. Yang, P. N. Rudd, Y. C. Shao, X. Z. Dai, H. T. Wei, J. J. Zhao, Y. J. Fang, Q. Wang, Y. Liu, Y. H. Deng, X. Xiao, Y. X. Feng and J. S. Huang, *Sci. Adv.*, 2019, **5**, eaav8925.
2. M. M. Tavakoli, M. Saliba, P. Yadav, P. Holzhey, A. Hagfeldt, S. M. Zakeeruddin and M. Gratzel, *Adv. Energy Mater.*, 2019, **9**, 1802646.